Molecular Dynamics Simulation of Nanoparticle Chain Aggregate Sintering

Takumi Hawa[1,2] and Michael R Zachariah[1,2]
[1]University of Maryland, College Park, MD, 20742
[2]National Institute of Standards and Technology, Gaithersburg, MD, 20899

ABSTRACT

Sintering of silicon nanoparticle chain aggregates are investigated using molecular dynamics (MD) simulations at 1500 K, which is about melting temperature at the size range we tested. The straight chain aggregates consist of upto 40 particles and the primary particles of 2.5 to 5 nm sizes are considered. The sintering time increases with increase the total volume of the chain aggregate or with increase the exposed initial surface area of the chain. A mathematical model was developed to describe the dynamics of sintering of chain aggregates. The model was able to predict the sintering time with excellent agreement with the results obtained from MD simulations. We also studied the chain aggregate that has a secondary branch coming out from the edge of the primary branch (L-shape) and from the middle of the primary branch (T-shape). In general, sintering time changes as much as 30% of that of a straight chain which contains the same volume of particles.

INTRODUCTION

Fabrication of the desired size with a narrow size distribution, and desired structure, is seen as one of the major challenge in robust implementation of nanoscience to a nanotechnology. The two most obvious ways to control the size of primary particles grown from the vapor are to either change the characteristic collision time by dilution or change the coalescence time by changing particle temperature.

For large scale production or for ultraclean materials, a gas phase production method is generally the method of choice [1-4]. Aerosol synthesis however, typically results in highly aggregated structures. The size of the spherical primary particles and the growth of agglomerates are determined by the rate of collision and subsequent sintering of particles. To understand the dynamics it would be useful to understand how aggregates sinter.

Several researchers have approached the problem of aggregate sintering using Monte-Carlo [5, 6] or other Brownian dynamics approaches [7]. However, all previous approaches were simulated by making assumptions as to how sintering would occur in an aggregate, and then applying a standard sintering approach to map the evolution of the morphology.

Our approach is to investigate how this aggregate sintering is actually taking place by use of atomistic simulation, and probe how it might differ from the simplest case of binary particles. We use the results to obtain both insight, and a better approach to phenomenologically modeling aggregate particle sintering. To the best of our knowledge, there is no MD work that has investigated the sintering of nanoparticle aggregate chains.

In this paper we focus on the simplest geometric representation of an aggregate, that of a chain of particles of equal primary particle size. We will use MD simulation to track

the evolution of a sintering process and compute the sintering time. We will also present a mathematical model of nanoparticle chain aggregates based on the assumption of viscous flow. We clarify the relationship between chain length and the primary particle size in the dynamics of sintering, and provide insight into the relationship between the mathematical model, and the MD simulation results, and identify the mechanism of sintering for straight chained aggregates.

MATHEMATICAL MODEL FOR AGGREGATE SINTERING

We consider the coalescence of a finite number of particles aligned in a straight line, that are initially in contact with each other. We assume that the coalescence of a chain aggregate is dominated by a contraction of cylinder in axial direction, and neglect the initial (minimization of surface defects) and final (convergence to a sphere) processes from our mathematical model for simplicity.

In the coalescence model we also assume that the chain aggregates retain its shape as a column during the coalescence. From the balance of viscous dissipation and work done by surface tension, we obtain the following expression for the velocity gradient parameter α:

$$\alpha = -\frac{\sigma}{3\eta r}\left[1+\frac{1}{2}\left(\frac{r}{L}\right)\right].$$ (1)

where η is the viscosity, σ is surface tension, r is a radius of the cylinder, and L is the length of the cylinder. Integrating over the entire process of the coalescence, which is the initial chain length, L_0, to $(4V/\pi)^{1/3}$. i.e. when the diameter of the cylinder is equal to the length of the cylinder, where V is the total volume of the column, gives

$$t = \frac{\eta}{\sigma}\left(\frac{2V}{\pi}\right)^{1/3}(A+B+C),$$ (2)

where

$$A = -2\sqrt{3}\left\{\mathrm{Atan}\left[\frac{1-2^{5/3}}{\sqrt{3}}\right] - \mathrm{Atan}\left[\frac{1-2\left(2\sqrt{\pi/V}\right)^{1/3}\sqrt{L_0}}{\sqrt{3}}\right]\right\},$$

$$B = -2\left\{\ln\left[1+2^{2/3}\right] - \ln\left[1+\left(2\sqrt{\frac{\pi}{V}}\right)^{1/3}\sqrt{L_0}\right]\right\}, \text{ and}$$

$$C = \ln\left[1-2^{2/3}+2^{4/3}\right] - \ln\left[1-\left(2\sqrt{\frac{\pi}{V}}\right)^{1/3}\sqrt{L_0}+\left(2\sqrt{\frac{\pi}{V}}\right)^{2/3}L_0\right].$$

## COMPUTATIONAL MODEL AND SIMULATION PROCEDURE

This study also involves atomistic simulations using classical MD. For this work we use the Stillinger-Weber interatomic potential for the silicon system [8]. All simulations

are run on the JVN computer in the Army High Performance Computer Research Center running up to 32 processors. Atom trajectories are determined by the velocity form of the Verlet algorithm [9], and time steps of 0.5 fs are typically used. The Verlet neighbor list with parallel architecture is also employed in all the simulations. Particles of various sizes (2.5 to 5 nm) (500 to 4000 Si atoms) at 1500 K are prepared, and duplicated particles are placed on a straight line, L- and T-shape initially in contact with each other.

RESULTS AND DISCUSSIONS

Long Chain Aggregate

Fig. 1 shows the temporal variation of the particle morphology for a 40 particle chain aggregate of primary particles of 500 Si atoms (Fig. 1(a)). The chain aggregate initially develops a smooth surface curvature, and forms a cylinder like shape (Fig. 2(b)). As it can be seen in Fig. 1(c), that as the cylinder begins to shrink mass accumulates at the ends of the rod, in the form of a dumbbell. Basically what is happening is that atoms in the center of the cylinder are being pulled by neighbors on either axial side, while atoms at the end of the aggregate have neighbors only to one side. So that as the aggregate tries to shrink it is easier for the end of the rod to grow. The morphological progression to a sphere is presented in the successive images (Fig. 1(e, f, g)).
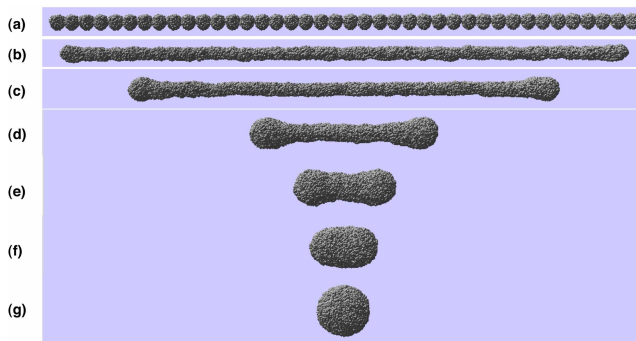
**Figure 1.** Temporal snapshots of the morphology of a 40 particle chain aggregate.
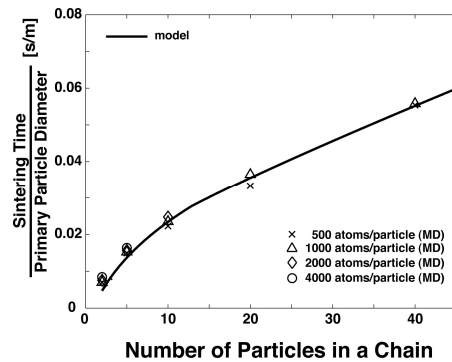
Figure 2. Sintering time per primary particle diameter vs. as number of particles in a chain.

We plot the MD simulated sintering time of the chain normalized by primary particle diameter, vs. number of primary particles in the chain, for 500, 1000, 2000, and 4000 atoms per primary particle in Fig. 2. The choice of plotting the MD results in terms of a normalized sintering time is based on our phenomenological model sintering time, expressed in Eq. (2), which shows a linear dependence on diameter. The data points correspond to the MD simulations and indicate a monotonic increase in sintering time with increasing chain length or primary particle diameter for all sizes of primary particles. By plotting the normalized sintering time we obtain results that are independent of primary particle diameter and only depend on the number of primary units. A comparison with the phenomenological model for the case of 500 atoms/particle is shown as a solid line in the figure. Our model shows excellent agreement for all lengths and sizes of chain aggregates.
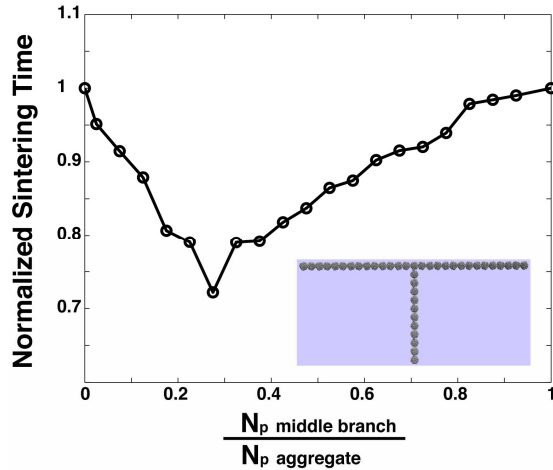
L- and T-shaped Aggregate

Sintering time as a function of ratios of secondary to primary branch length is summarized in Figure 3, for an aggregate of 40 primaries of 500 atoms each. The normalized sintering time is defined relative to the corresponding straight chain aggregate containing the same number of total primary particles. It shows that the L-shape structure does not affect to total sintering time, whose deviation is within ± 4.5%. This results indicate that the L-shape aggregate, behaves much like a straight chain, and thus the effective primary branch is the total length of the L-shape aggregate.

Sintering time as a function of ratios of number of particles in a middle branch to an entire aggregate is summarized in Figure 4. Vertical axis is the sintering time normalized by the straight chain aggregate containing the same number of total primary particles (40). When the middle branch is short, the sintering process of the T-shape aggregate approximated as that of straight chain aggregate with a small disturbance at the middle. Thus, the sintering time is determined by the initial length of the primary branch. The minimum sintering time is about the 70 % of the straight chain aggregate containing the same number of total primary particles and found at the ratio of 0.28, which is slightly smaller than the 0.33 which corresponds to the middle branch, top and bottom portion of the primary branches of equal length. Above the critical ratio of 0.28, the sintering time monotonically increases with the ratio.
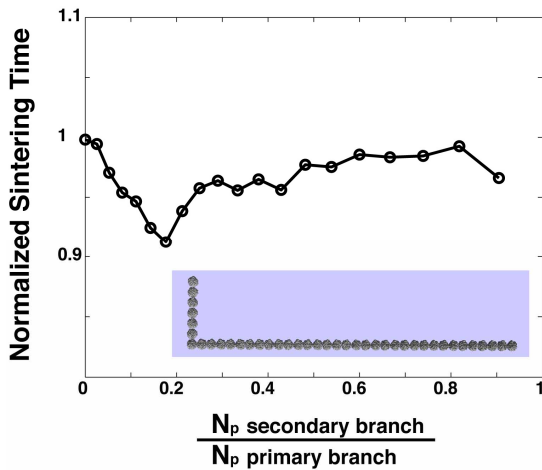
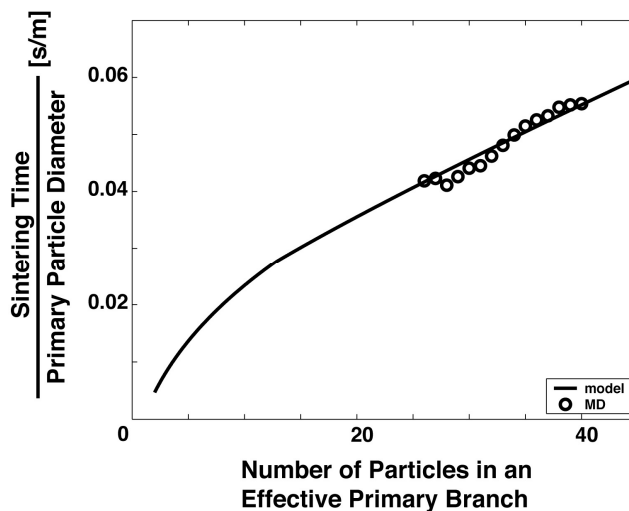**Figure 3.** Sintering time of L-shaped aggregates.   **Figure 4.** Sintering time of T-shaped aggregates.

Both L- and T-shape aggregate studies indicate that the primary branch length determines the sintering time. What determines the definition of the primary branch, is the longest contiguous chain length. In some cases for the T-shaped aggregate this might be the vertical of the T and half the horizontal, if the vertical is longer than the horizontal.

We plot the sintering time of the T-shape aggregate normalized by primary particle diameter as a function of number of particles in an effective primary branch in Fig. 5. The solid line represents the sintering time for straight chain aggregates obtained from the model Eq. (2) of the viscous flow equation. MD simulation results show excellent agreement with the viscous flow model. This indicates that the effective primary branch

length dominates the sintering process of the simple chain aggregates, and that secondary branches are small disturbance to the primary branch.

Figure 5. A comparison of MD sintering time of T-shaped aggregates normalized by primary particle diameter with a viscous flow model for a chain aggregate.

CONCLUSIONS

Classical MD with the Stillinger-Weber potential was used to study the sintering of chain aggregates of silicon nanoparticles. Simulations were performed over a wide range of particle diameters (a) between 2.5 - 5 nm at a length between 2 – 40 particle chain, for straight, L- and T-shaped aggregates. The sintering time increases with increase the total volume of the chain aggregate or with increase the exposed initial surface area of the chain. A mathematical model was developed to describe the dynamics of sintering of chain aggregates. The model was able to predict the sintering time with excellent agreement with the results obtained from MD simulations. We also studied the chain aggregate that has a secondary branch coming out from the edge of the primary branch (L-shape) and from the middle of the primary branch (T-shape). In general, sintering time changes as much as 30% of that of a straight chain which contains the same volume of particles. Their sintering time was predicted from the viscous flow model based on the effective primary branch length.

ACKNOWLEDGEMENTS

REFERENCE

1. F.E. Kruis, H. Fissan, and A. Peled, *Journal of Aerosol Science*, **29**, 5/6 (1998)
2. C. Artelt, H.J. Schmid, and W. Peukert, *Journal of Aerosol Science*, **36**, (2004)
3. S.K. Friedlander and M.K. Wu, *Physical Review B*, **49**, 5 (1994)
4. J. Frenkel, *Journal of Physics*, **9**, 5 (1945)

5. M.K. Akhtar, G.G. Lipscomb, and S.E. Pratsinis, *Aerosol Science and Technology*, **21**, (1994)
6. H.J. Schmid, S. Tejwani, C. Artelt, and W. Peukert, *Journal of Nanoparticle Research*, **6**, (2004)
7. P. Kulkarni and P. Biswas, *Journal of Nanoparticle Research*, **5**, (2003)
8. F.H. Stillinger and T.A. Weber, *Physical Review B*, **31**, (1985)
9. L. Verlet, *Phys. Rev. B*, **159**, (1967)